

Ultimate low loss of hollow-core photonic crystal fibres

P. J. Roberts, F. Couny, H. Sabert, B. J. Mangan, D. P. Williams, L. Farr, M. W. Mason and A. Tomlinson

BlazePhotonics Ltd, University of Bath Campus, Claverton Down, Bath BA2 7AY, United Kingdom

T. A. Birks, J. C. Knight and P. St.J. Russell

Department of Physics, University of Bath, Claverton Down, Bath BA2 7AY, United Kingdom

pystab@bath.ac.uk

<http://www.bath.ac.uk/physics/groups/ppmg/>

Abstract Hollow-core photonic crystal fibres have excited interest as potential ultra-low loss telecommunications fibres because light propagates mainly in air instead of solid glass. We propose that the ultimate limit to the attenuation of such fibres is determined by surface roughness due to frozen-in capillary waves. This is confirmed by measurements of the surface roughness in a HC-PCF, the angular distribution of the power scattered out of the core, and the wavelength dependence of the minimum loss of fibres drawn to different scales.

©2005 Optical Society of America

OCIS codes: (060.2280) Fiber design and fabrication, (230.4000) Microstructure fabrication

References and links:

1. P. St.J. Russell, "Photonic crystal fibers," *Science* **299**, 358-362 (2003).
2. R. F. Cregan, B. J. Mangan, J. C. Knight, T. A. Birks, P. St.J. Russell, P. J. Roberts and D. C. Allan, "Single-mode photonic band gap guidance of light in air," *Science* **285**, 1537-1539 (1999).
3. C. M. Smith, N. Venkataraman, M. T. Gallagher, D. Müller, J. A. West, N. F. Borrelli, D. C. Allan and K. W. Koch, "Low-loss hollow-core silica/air photonic bandgap fibre," *Nature* **424**, 657-659 (2003).
4. J. A. West, C. M. Smith, N. F. Borrelli, D. C. Allan and K. W. Koch, "Surface modes in air-core photonic band-gap fibers," *Opt. Express* **12**, 1485-1496 (2004), <http://www.opticsexpress.org/abstract.cfm?URI=OPEX-12-8-1485>.
5. B. J. Mangan, L. Farr, A. Langford, P. J. Roberts, D. P. Williams, F. Couny, M. Lawman, M. Mason, S. Coupland, R. Flea, H. Sabert, T. A. Birks, J. C. Knight and P. St.J. Russell, "Low loss (1.7 dB/km) hollow core photonic bandgap fiber," in *Proc. Opt. Fiber. Commun. Conf.* (2004), paper PDP24.
6. K. Nagayama, M. Kakui, M. Matsui, I. Saitoh and Y. Chigusa, "Ultra-low-loss (0.1484 dB/km) pure silica core fibre and extension of transmission distance," *Electron. Lett.* **38**, 1168-1169 (2002).
7. T. Miya, Y. Terunuma, T. Hosaka and T. Miyashita, "Ultimate low-loss single-mode fibre at 1.55 μm ," *Electron. Lett.* **15**, 106-108 (1979).
8. M. Ohashi, K. Shiraki and K. Tajima, "Optical loss property of silica-based single-mode fibers," *IEEE J. Lightwave Technol.* **10**, 539-543 (1992).
9. M. K. Sanyal, S. K. Sinha, K. G. Huang and B. M. Ocko, "X-ray-scattering study of capillary-wave fluctuations at a liquid surface," *Phys. Rev. Lett.* **66**, 628-631 (1991).
10. A. K. Doerr, M. Tolan, W. Prange, J.-P. Schlomka, T. Seydel, W. Press, D. Smilgies and B. Struth, "Observation of capillary waves on liquid thin films from mesoscopic to atomic length scales," *Phys. Rev. Lett.* **83**, 3470-3473 (1999).
11. T. Seydel, A. Madsen, M. Tolan, G. Grübel and W. Press, "Capillary waves in slow motion," *Phys. Rev. B* **63**, 073409 (2001).
12. J. Jäckle and K. Kawasaki, "Intrinsic roughness of glass surfaces," *J. Phys.: Condens. Matter* **7**, 4351-4358 (1995).
13. P. K. Gupta, D. Inmiss, C. R. Kurkjian and Q. Zhong, "Nanoscale roughness of oxide glass surfaces," *J. Non-Cryst. Solids* **262**, 200-206 (2000).
14. R. Brückner, "Properties and structure of vitreous silica I," *J. Non-Cryst. Solids* **5**, 123-175 (1970).
15. N. P. Bansal and R. H. Doremus, *Handbook of Glass Properties* (Academic Press, Orlando, 1986).
16. A. W. Snyder and J. D. Love, *Optical Waveguide Theory* (Chapman and Hall, London, 1983).

17. J. D. Joannopoulos, R. D. Meade and J. N. Winn, *Photonic Crystals* (Princeton University Press, Princeton, 1995).
18. F. P. Payne and J. P. R. Lacey, "A theoretical analysis of scattering loss from planar optical waveguides," *Opt. Quantum Electron.* **26**, 977-986 (1994).
19. A. Roder, W. Kob and K. Binder, "Structure and dynamics of amorphous silica surfaces," *J. Chem. Phys.* **114**, 7602-7614 (2001).
20. A. D. Fitt, K. Furusawa, T. M. Monro, C. P. Please and D. J. Richardson, "The mathematical modelling of capillary drawing for holey fibre manufacture," *J. Eng. Math.* **43**, 201-227 (2002).
21. A. L. Yarin, P. Gospodinov, V. I. Roussinov, "Stability loss and sensitivity in hollow fiber drawing," *Phys. Fluids* **6**, 1454-1463 (1994).
22. M. E. Lines, W. A. Reed, D. J. Di Giovanni and J. R. Hamblin, "Explanation of anomalous loss in high delta singlemode fibres," *Electron. Lett.* **35**, 1009-1010 (1999).
23. F. Couny, H. Sabert, P. J. Roberts, D. P. Williams, A. Tomlinson, B. J. Mangan, L. Farr, J. C. Knight, T. A. Birks and P. St.J. Russell, "Visualization of the photonic band gap in hollow core photonic crystal fibers using side scattering," submitted to *Opt. Express*.
24. Hecht, J. *Understanding Fiber Optics* (Prentice Hall, Columbus, 1999).
25. N. M. Litchinitser, A. K. Abeeluck, C. Headley and B. J. Eggleton, "Antiresonant reflecting photonic crystal optical waveguides," *Opt. Lett.* **27**, 1592-1594 (2002).
26. A. Kucuk, A. G. Clare and L. Jones, "An estimation of the surface tension for silicate glass melts at 1400 °C using statistical analysis," *Glass Technol.* **40**, 149-153 (1999).
27. N. M. Parikh, "Effect of atmosphere on surface tension of glass," *J. Am. Ceram. Soc.* **41**, 18-22 (1958).
28. S. D. Hart, G. R. Maskaly, B. Temelkuran, P. H. Pridaux, J. D. Joannopoulos and Y. Fink, "External Reflection from Omnidirectional Dielectric Mirror Fibers," *Science* **296**, 510-513 (2002).
29. K. Kuriki, O. Shapira, S. D. Hart, G. Benoit, Y. Kuriki, J. F. Viens, M. Bayindir, J. D. Joannopoulos and Y. Fink, "Hollow multilayer photonic bandgap fibers for NIR applications," *Opt. Express* **12**, 1510-1517 (2004), <http://www.opticsexpress.org/abstract.cfm?URI=OPEX-12-8-1510>.

1. Introduction

Hollow-core photonic crystal fibres (HC-PCFs) are optical fibres with claddings made of glass (usually fused silica) incorporating arrays of air holes, Fig. 1. The core is formed by omitting several unit cells of material from the cladding. The "holey" cladding has a two-dimensional photonic bandgap that can confine light to the core for wavelengths around a minimum-loss wavelength I_c , even when the core is hollow and filled with air [1-5]. In contrast, a conventional fibre guides light by total internal reflection so its core must have a higher refractive index than the cladding.

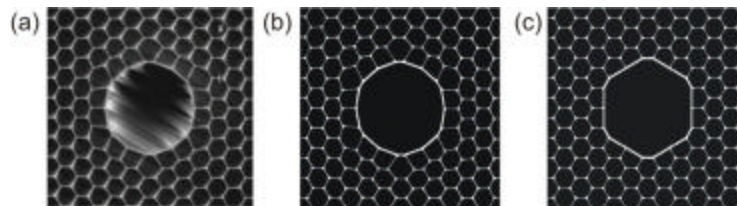


Fig. 1. (a) Scanning electron micrograph (SEM) of the 1.7 dB/km HC-PCF with a 20 μm diameter core (the 1.2 dB/km fibre discussed in the text was very similar), (b) a digitised representation used for modelling and (c) a similar but idealised structure with lower predicted loss.

The minimum optical attenuation of ~ 0.15 dB/km in conventional fibres [6] is determined by fundamental scattering and absorption processes in the high-purity glass [7,8], leaving little prospect of much improvement. However, over 99% of the light in HC-PCFs can propagate in air [5] and avoid these loss mechanisms, making HC-PCFs promising candidates as future ultra-low loss telecommunication fibres. Nevertheless the lowest loss reported in HC-PCFs is 1.7 dB/km [5], though we have since reduced this to 1.2 dB/km. An understanding of the fundamental limitations to this loss is therefore of great importance.

Direct leakage of light from the core is easily suppressed by incorporating enough holes in the cladding [4]. Fibre nonuniformity then becomes the key loss mechanism, coupling or scattering light from the guided "fundamental" mode [3,4]. Fluctuations of technological

origin can be reduced by more careful fibre fabrication. However, surface roughness from surface capillary waves (SCWs) frozen into the fibre as it is made [9-13] is inevitable because of its thermodynamic origin. We propose that it ultimately limits the attenuation of HC-PCFs, and derive three experimentally-testable consequences. In all three cases the predictions are confirmed, demonstrating that the attenuation of our fibres is already dominated by this mechanism. We discuss the implications for the minimum attenuation possible in HC-PCF.

2. Modelling

2.1 Surface roughness due to SCWs

SCWs exist on liquid surfaces (like molten glass) where surface tension provides a restoring force. Short-wavelength ripples in water are a familiar example. It follows from equipartition of energy that each SCW mode at thermal equilibrium has average energy $\frac{1}{2}k_B T$, where k_B is Boltzmann's constant and T the temperature [9,10]. As a glass solidifies the SCWs freeze [11], leaving a surface roughness given by the SCW amplitudes when T is the glass transition temperature T_g [12,13].

The 1-D statistical spectral density $S_z(\mathbf{k})d\mathbf{k}$ is the mean square amplitude of roughness components with spatial frequencies along the fibre between \mathbf{k} and $\mathbf{k}+d\mathbf{k}$. It is evaluated by integrating the corresponding 2-D expression [12] over the transverse co-ordinate. (A more thorough treatment including the azimuthal roughness distribution is much more complicated, and yields results little different from the ones derived below.) For an unbounded flat surface

$$S_z(\mathbf{k}) = \frac{k_B T_g}{4\pi g k}, \quad (1)$$

where g is the surface tension. (Note that $S_z(\mathbf{k})$ in Eq. (1) is scale-free; it describes a fractal surface with no correlation length.) Closure of the surface to form a cylindrical hole of perimeter W quantises the SCW modes transversely, and the same procedure leads to

$$S_z(\mathbf{k}) = \frac{k_B T_g}{4\pi g k} \coth\left(\frac{kW}{2}\right), \quad (2)$$

which reduces to Eq. (1) for small length scales (large \mathbf{k}).

$S_z(\mathbf{k})$ in Eqs. (1) and (2) diverges for small \mathbf{k} . In other situations this is prevented by long-scale cutoffs arising from gravity [12] or a substrate [10]. For thin free structures like HC-PCFs the physical origins of any analogous cutoff are unclear, but it is reasonable to assume it is large compared to W and scales with the fibre's dimensions. Importantly, inclusion of such a cutoff does not affect the dimensional argument leading to Eq. (7).

Eq. (2) describes the statistics of the surface roughness. On integration the rms roughness over a decade of length scales small compared to W is just ~ 0.1 nm in fused silica ($T_g \sim 1500$ K, $g = 0.3$ Jm⁻² [14,15]), but this is enough to dominate the loss of our fibres.

2.2 Dependence on effective index

The surface roughness scatters light from the fundamental mode to other modes that are not guided. This can be described by coupled mode theory [16] in terms of the modal effective index $n = \mathbf{b}/k$, where \mathbf{b} is the propagation constant and $k = 2\pi/\lambda$. Light is coupled between modes with effective indices n_0 (the fundamental mode) and n by the roughness component with spatial frequency

$$\mathbf{k} = k |n - n_0|, \quad (3)$$

at a rate determined by $S_z(\mathbf{k})$ and an overlap integral of both modes on the glass-air surfaces in the fibre's cross-section. The overall loss is the statistical sum of the power coupled to the modes. A full calculation is prohibitively complicated, requiring field distributions and \mathbf{b} for

many cladding and radiation modes as well as other core-guided and surface modes [4]. However, for values of n away from n_0 and hence the bandgap, the effects of the photonic band structure wash out. To a good approximation the overlap integrals average out over groups of modes with similar n , and become proportional to a constant F quantifying the overlap of just the fundamental mode with the surfaces:

$$F = \left(\frac{\epsilon_0}{\mu_0} \right)^{1/2} \frac{\oint_{\text{hole perimeters}} dl |\mathbf{E}|^2}{\int_{\text{cross-section}} dA \mathbf{E} \times \mathbf{H}^* \cdot \hat{\mathbf{z}}}, \quad (4)$$

where \mathbf{E} and \mathbf{H} are the electric and magnetic field distributions respectively of the fundamental mode and $\hat{\mathbf{z}}$ is the unit vector along the fibre. Furthermore in this case $S_z(\mathbf{k})$ has the simplified form of Eq. (1), so the scattering loss response is

$$\mathbf{a}_n(n) \propto \frac{F}{|n - n_0|}, \quad (5)$$

where $\mathbf{a}_n(n)dn$ is the fraction of power scattered per unit length into modes with effective indices between n and $n+dn$. This equation describes the scattered intensity as a function of effective index and hence of the direction of scattering.

Although we could not calculate absolute attenuation for a realistic fibre, we did perform the simpler calculation for scattering from the (leaky) hollow-core mode of a thin cylindrical shell in air. The result matched experiment to within a factor of 2. Roughness due to SCWs therefore appears to be responsible for most of the loss in our HC-PCFs, so the major technological sources of loss must be close to being eliminated.

2.3 Dependence on wavelength

If the transverse scale of a HC-PCF changes without otherwise changing the fibre's structure, the wavelength I_c of minimum attenuation must scale in proportion [2,17]. Without recourse to the approximations of the previous section, the mean square amplitude of the roughness component that couples light into modes with effective indices between n and $n+dn$ is

$$u^2 = \frac{k_B T}{4\mu_0 g(n - n_0)} \coth\left(\frac{(n - n_0)kW}{2}\right) dn \quad (6)$$

from the definition of $S_z(\mathbf{k})$ and Eqs. (2) and (3). This has units of length squared, and is independent of I_c because we scale W so that kW is constant. The attenuation to these modes is proportional to u^2 [16,18] but the only other independent length scale it can vary with is I_c . As attenuation has units of inverse length, it must therefore by dimensional analysis be inversely proportional to the cube of I_c . If this is true for every set of destination modes, it must be true for the net attenuation \mathbf{a} to all destination modes, so

$$\mathbf{a}(I_c) \propto \frac{1}{I_c^3}. \quad (7)$$

This equation (described phenomenologically in [5] but without theoretical support) predicts the attenuation of a given fibre drawn to operate at different wavelengths. The result differs from the familiar $1/I^4$ dependence of Rayleigh scattering in bulk media [7], and importantly applies to inhomogeneities at all length scales not just those small compared to I .

3. Experimental results

We carried out three experiments to test whether the SCW mechanism explains the loss properties of our HC-PCFs.

3.1 AFM measurement of surface roughness

We directly measured surface roughness inside a HC-PCF using an atomic force microscope (AFM) [13]. The fibre was crushed and the wall of a 3 μm diameter hole identified among the fragments that resulted. 64 scans of the AFM probe over 10 μm lengths along the original direction of the fibre were made at well-separated locations within the hole. The spectral density $S_z(\mathbf{k})$ was calculated from the measured height profiles after compensating for the nonlinear response of the AFM. Some large spikes in the data were due to electrical noise at known identifiable temporal frequencies and were not representative of the roughness spectrum. The accuracy of the first few low spatial frequency points was compromised by the limited scan length, and the high-frequency cutoff of the AFM was about 20 μm^{-1} .

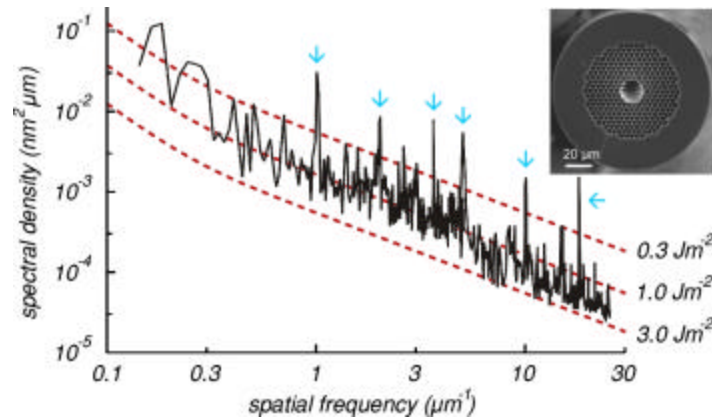


Fig. 2. (solid line) The roughness spectrum measured by AFM along a hole in a HC-PCF. The arrows identify artefacts due to electrical noise. (broken red lines) Roughness spectra calculated from Eq. (2) for three values of surface tension. (inset) SEM of the endface of the HC-PCF with a 19-cell core and an attenuation of 1.7 dB/km at 1565 nm wavelength.

The spectral density $S_z(\mathbf{k})$ is plotted in Fig. 2, with the predictions of Eq. (2) for different surface tensions g . The measurement fits the equation over two orders of magnitude in length scale for g around 1.0 Jm^{-2} , somewhat larger than the commonly quoted value of 0.3 Jm^{-2} for fused silica [15]. The discrepancy is not due to other roughening mechanisms because the roughness is actually smaller than predicted, and SCWs certainly do contribute to roughness [12,13]. Instead it indicates that g inside the fibre is indeed larger.

This does not contradict previous measurements of g because they were not made for fused silica under modern fibre fabrication conditions. The theoretical g for silica determined from bond energies is 5.2 Jm^{-2} , measured values being lower because real surfaces become covered with silanol (SiOH) groups after formation [15]. Fibre fabricators take great care to eliminate OH (a source of absorption loss) from their processes, coincidentally reducing the silanol concentration and so raising g . Other calculations [19] predict lower theoretical values for g without silanol, but the upper bound obtained by extrapolation to T_g still exceeds 1.4 Jm^{-2} and so accommodates our measurement. Furthermore we independently measured g while drawing silica capillaries, by finding the pressure in the hole that balances collapse due to surface tension [20], and also found a raised value (0.7 Jm^{-2} in that case).

We have therefore not only measured a roughness spectrum consistent with SCWs as the cause, but also found that surface tension can be considerably greater than usually assumed. This is significant because g determines the stability of fibre drawing, especially in structures with holes [20,21]. The beneficial effects of raising g make the removal of OH from HC-PCFs more important for reducing loss than hitherto realised.

3.2 Angular-resolved scattering measurements

We performed angular-resolved scattering measurements [22,23] on the fibre of Fig. 1(a), with a 20 μm diameter core formed by omitting 19 unit cells from a cladding of 3.9 μm pitch. One of our lowest-loss fibres, its attenuation was 1.7 dB/km at 1565 nm wavelength [5]. Laser light of 1550 nm wavelength was coupled into the fibre, taking care to minimise excitation of modes other than the fundamental. Over 100 m of input fibre ensured that transient leaky modes decayed away before reaching 5.5 mm of fibre that was stripped of its coating. This was mounted centrally across the diameter of a 32-mm diameter cylindrical vessel filled with index-matching fluid of index $n_f = 1.449$. Stray light from the rest of the fibre (ie other than the 5.5 mm stripped section) was shielded by black tubing.

Light emerging from the vessel was focused onto a photodetector array. By repeated rotation of the sample, we could measure the light leaking from the fibre as a function of direction over all angles \mathbf{q} to the fibre axis. This was converted to $P(n)$, where $P(n)dn$ is the power lost to modes with effective index between n and $n+dn$, using the relationship $n = n_f \cos \mathbf{q}$ and accounting for the appropriate geometrical factors. The net attenuation due to scattering should be simply the integral of $P(n)dn$.

A typical measurement of $P(n)$ is plotted in Fig 3; similar measurements on other sections of fibre several metres away yielded almost identical curves. Integration over all n yields a net leakage rate of 2 dB/km, matching within experimental error the 1.7 dB/km measured by the cut-back technique. Hence the fibre's loss is primarily due to scattering not absorption, and is uniform along its length down to the mm scale.

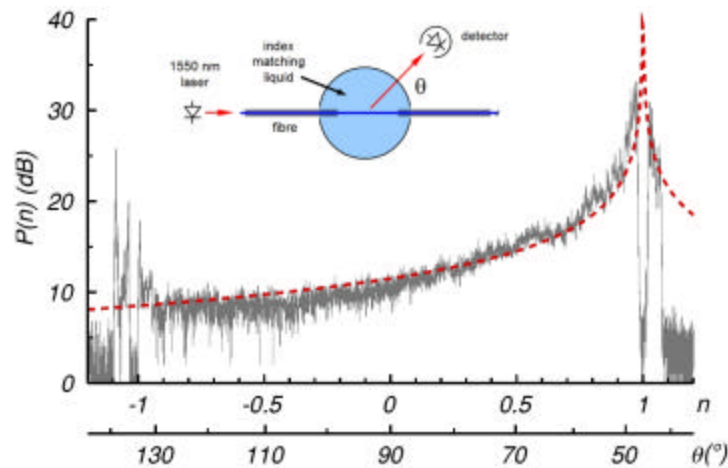


Fig. 3. The power $P(n)$ per unit effective index n scattered from 5.5 mm of HC-PCF into fluid of index $n_f = 1.449$, as a function of n and of scatter angle \mathbf{q} . The solid grey curve is from measured data and the broken red curve is a fit to Eq. (5). The vertical origin is arbitrary. (inset) Schematic diagram of the experimental setup.

A bandgap, where guided modes but not cladding modes exist, is evident around $n = 1$. The measured power falls to the experimental noise floor, confirming negligible direct tunnelling from the fundamental mode. Instead, light must be scattered into other modes by inhomogeneities before leaking out. Hence Fig. 3 represents the variation with n of scattering strength from the fundamental mode; ie $P(n) \propto \mathbf{a}_n(n)$.

$P(n)$ finally cuts off around $n = 1.07$, agreeing with computations of the cladding's maximum effective index. The graph shows considerable structure around the bandgap but for smaller n it follows a steady tail as n decreases until the bandgap for backward waves around $n = -1$. A fit to Eq. (5) is also shown and where it is valid (ie away from the bandgaps) closely models the data, confirming that the experiment is consistent with SCWs being the cause of surface roughness.

3.3 Attenuation spectra

We measured attenuation spectra by the cut-back technique [24]. A cut-back length of at least 50 m allowed transient leaky modes to decay away, so that only the fundamental mode is measured. For a set of similar HC-PCFs we determined the minimum attenuation as a function of the wavelength I_c of the minimum. The fibres had 7-cell cores but were drawn to different scales, giving them different I_c but otherwise comparable properties [2,17]. The minimum attenuation is plotted in Fig. 4 against I_c on a log-log scale. A straight-line fit is shown and has a slope of -3.07 , supporting the predicted inverse cubic dependence in Eq. (7).

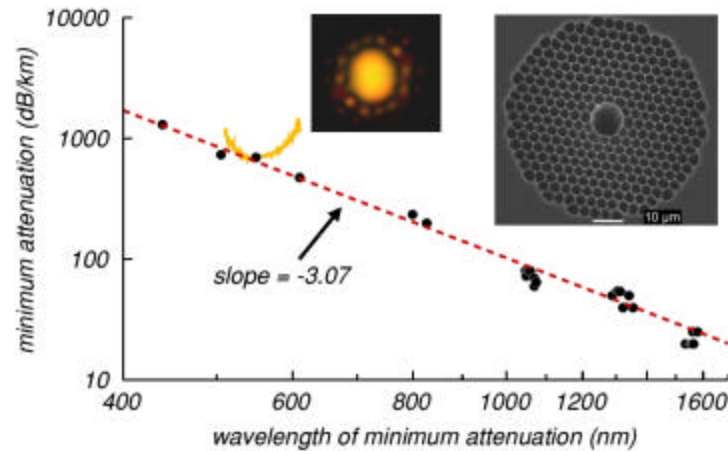


Fig. 4. (solid orange curve) The low-loss part of the measured attenuation spectrum of a 7-cell HC-PCF, with a minimum of 700 dB/km at $I_c = 550$ nm. (left inset) Measured near-field pattern at the output of this fibre at 550 nm. (points) The minimum attenuation of similar HC-PCFs with various transverse scales, versus the wavelength I_c of minimum attenuation. (broken red line) A straight-line fit to the points, having a slope of -3.07 . (right inset) SEM of a representative of these HC-PCFs, with $I_c \approx 1550$ nm.

4. Reducing the attenuation of HC-PCFs

Our results imply that surface roughness due to frozen-in SCWs is already limiting HC-PCF attenuation. If so, given its thermodynamic origin, it cannot be reduced much further simply by improving the fibre drawing process. For example, changing draw speed and tension made no appreciable difference to the roughness characteristics. We expect remaining technological improvements in homogeneity to reduce the attenuation of fibres like that in Fig. 1 by no more than a factor of two. Instead, having gained an understanding of its properties, we outline approaches to mitigate the effects of SCW-induced roughness.

4.1 Fibre design

F in Eqs. (4) and (5) can be minimised by designing the fibre to reduce the overlap of the fundamental mode with the glass-air surfaces. For example our modelling work indicates that minimum F varies roughly as the inverse cube of the core diameter, if the cladding and the core boundary are otherwise unchanged. This matches the scaling of F for a simple step-index fibre, derived from textbook results in the multimode limit [16]. Hence the reduction in reported attenuation from 13 dB/km [3] to 1.7 dB/km [5] (and now 1.2 dB/km) was partly from enlarging the core from 7 to 19 unit cells, reducing F by a factor of $(19/7)^{3/2} \approx 4.5$. (F could be further reduced by enlarging the core to 37 cells for example. However, this would be accompanied by propagation of more higher-order core modes, increased bending loss and

closer spectral packing of surface modes [4]. Since these are already apparent in our 19-cell HC-PCF [5], we expect 37-cell HC-PCFs to be of very limited practical value.)

The core boundary was also thickened relative to boundaries in the cladding (as evident in Fig. 1(a)) to give it anti-resonant properties [25] that expel light and further reduce F . We have extensively modelled different HC-PCF designs, and found that straightening the boundaries (Fig. 1(c) compared to 1(b)) and increasing the air filling fraction can further reduce F by factors of ~ 2 and ~ 1.5 respectively. Hence realistic and incremental changes to fibre design (and the factor of ~ 2 improvement we expect by eliminating remaining technological sources of loss) could plausibly reduce attenuation to ~ 0.2 dB/km.

4.2 Choice of operating wavelength

Longer operating wavelengths reduce scattering loss, but infrared absorption losses will rise because some light does propagate in the glass. The wavelength dependence of the minimum overall attenuation can be estimated [5] if the fraction f_a of light propagating in air is known. The attenuation due to absorption and Rayleigh scattering in bulk glass (estimated using a published approximate fit [8]) is multiplied by the fraction $(1 - f_a)$ of the light that is in the glass, calculated for the representative model structures of Fig. 1(b) and (c). The attenuation due to surface scattering is extrapolated from the measured minimum attenuation using Eq.

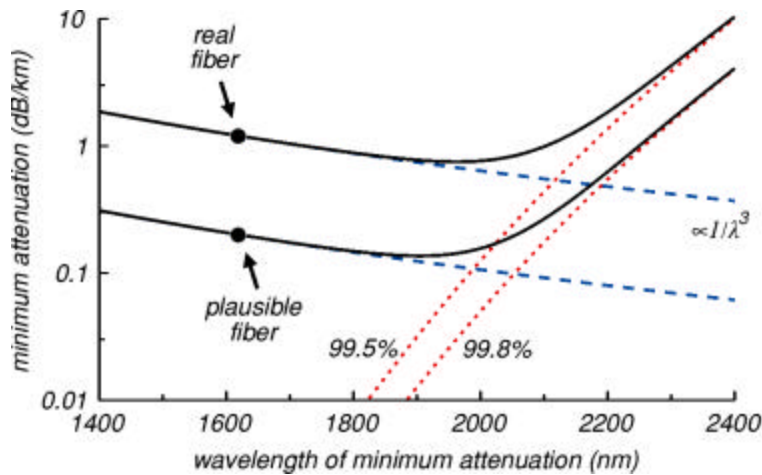


Fig. 5. Modelled bulk (dotted red lines) and surface (broken blue lines) contributions to the net (solid lines) minimum attenuation of 19-cell HC-PCFs, based on actual and plausible attenuation values at 1620 nm wavelength under the assumptions described in the text. Corresponding values of f_a are marked on the bulk attenuation curves.

(7). Their sum is an estimate of the minimum attenuation, absorption due to the air in the hole being negligible in comparison.

The minimum attenuation is plotted against wavelength in Fig. 5. When extrapolated from our existing fibre (1.2 dB/km at 1620 nm, $f_a = 99.5\%$) it falls to 0.75 dB/km at 1960 nm which is the loss the fibre would have if it had been made 21% bigger in diameter. The minimum attenuation based on the plausible fibre discussed above (0.2 dB/km at 1620 nm, $f_a = 99.8\%$) is 0.13 dB/km at 1900 nm, less than the best conventional fibres.

4.3 Reducing the SCW amplitudes

More speculatively, the SCW amplitudes of Eq. (2) may themselves be controlled. The T_g of silica cannot be reduced significantly, though other glasses have lower T_g . However, it may be possible to increase the surface tension g . Dry processing conditions seem to raise g by $3\times$ above the textbook value but the theoretical value is $5\times$ higher still [15], which would reduce

the minimum attenuation to ~ 0.03 dB/km. Although we do not suggest that such a high value of g could be attained in practice, it does imply some scope (and indeed motivation) to find material processes [26,27] that further increase g . Conversely, low g is desirable for reducing hole collapse when drawing fibre [20] but impacts adversely on surface roughness. Fibres made from solid materials with high index contrast but low interfacial tension could suffer greatly from enhanced surface inhomogeneities [28,29].

Finally, Eq. (5) and Fig. 3 show that long-scale (small k) roughness contributes most to surface scattering, including coupling to other guided modes and surface modes [4]. These roughness components are exaggerated by the coth factor in Eq. (2). Hence loss could be reduced by increasing the perimeter W of the core or adjacent holes. We found exotic designs with corrugated boundaries and inward protrusions that give significant calculated improvements, but they would be very difficult to realise experimentally.

5. Conclusions

The minimum loss in hollow-core photonic crystal fibres is limited by scattering due to surface roughness from frozen-in surface capillary waves. The attenuation of our best HC-PCFs, as low as 1.2 dB/km, appears to be already dominated by this mechanism. It can be mitigated through fibre design, and an attenuation of the order of 0.1 dB/km (less than the best conventional fibres) is plausible. Design improvements that we have not explored (such as the elimination of surface modes [4]), material processes to increase surface tension or alternative glasses transparent at longer wavelengths may further reduce the attenuation of HC-PCFs.

Acknowledgments

We thank Eli Yablonovitch for prompting us to explore SCWs as a possible source of surface roughness in PCFs.